Simultaneous Bi-Directional Structured Light Encoding for Practical Uncalibrated Profilometry

Torben Fetzer[1], Gerd Reis[2] and Didier Stricker[1,2]

[1] University of Kaiserslautern
[2] German Research Center for Artificial Intelligence (DFKI)
{torben.fetzer, gerd.reis, didier.stricker}@dfki.de

Abstract. Profilometry based on structured light is one of the most popular methods for 3D reconstruction. It is widely used when high-precision and dense models, for a variety of different objects, are required. User-friendly procedures encode the scene in horizontal and vertical directions, which allows a unique description of points in the scene. The resulting encoding, can be used to auto-calibrate the devices used. Thus, any consumer or industrial cameras or projectors can be supported and the procedure is not limited to pre-calibrated setups. This approach is extremely flexible, but requires a large number of camera acquisitions of the scene with multiple patterns projected. This paper presents a new approach that encodes the scene simultaneously in horizontal and vertical directions using sinusoidal fringe patterns. This allows to almost halve the number of recorded images, making the approach attractive again for many practical applications with time aspects.

Keywords: Structured Light · Reconstruction · Profilometry · Surface Encoding

1 Introduction

In the past decades, a multitude of different approaches for the creation of 3D reconstructions have been established. Basically, the procedures can be divided into active and passive procedures, which either directly affect the scene or not. In applications that require highly accurate and dense reconstructions of a wide variety of different objects, structured light approaches have become a preferred choice in industry. These methods usually illuminate the scene with specific patterns, e.g. stripes, pseudo-random-dots, etc. and use their interaction with the scene to estimate depth information. Particularly interesting are fringe projection strategies, where multiple horizontal and vertical sinusoidal patterns are projected onto the scene, in order to encode it in two directions. For cameras, capturing the fringe images, this enables the calculation of dense and robust correspondences (see [3]). This approach also works for un-structured and un-textured surfaces, where most passive methods fail due to the absence of necessary features. Depending on the required accuracy, the frequency of the projected fringes is increased

This work was partially funded by the projects MARMORBILD (03VP00293) and VIDETE (01W18002) of the German Federal Ministry of Education and Research (BMBF).

several times in order to successively improve the quality of the encoding. The high number of camera shots required, leads to a considerable expenditure of time in data acquisition, which is the main weakness of the method. To speed up the procedure, often, only one dimension is encoded with structured light and matches are found by intersection with corresponding epipolar lines. Unfortunately, this method is limited to calibrated devices, which means that replacing a camera, lens, changing the settings or moving a device leads to the considerable effort of re-calibration. Furthermore, accuracy often suffers, especially when lens distortions are taken into account. The method presented here, allows auto-calibrations due to the two-dimensional encoding, which makes it significantly more versatile and convenient to use.

According to the state of the art, the phase shifting method is the basis of most structured light methods, due to its texture-invariance. Thereby, sinusoidal fringe patterns with equidistantly shifted phases are projected onto the scene. A superposed phase, which can be calculated from at least three shifted patterns, encodes the scene pixel by pixel in the shifted direction. Doing this, both in horizontal and vertical direction, results in a minimum of 6 captured images. Even more acquisitions are necessary if further refinement steps with higher frequencies are performed. The patterns are sinusoidally modulated in the direction to be encoded and constantly continued in the decoded direction. Therefore, one dimension of the patterns does not carry any information, which is certainly a waste. In the following, more detailed investigations on the phase shifting algorithm and the harmonic addition theorem are carried out. Especially, findings with regard to the resulting amplitude of the phase superposition will encourage us to combine the horizontal and vertical stripe patterns in order to encode both directions simultaneously. The horizontal and vertical phases are then extracted from the combined patterns by a per pixel strategy, making the whole procedure scene-independent.

2 Related Work

Extensive research has been carried out in the field of structured light reconstruction. Various strategies, assuming pre-calibrated setups, have been reviewed and compared by Salvi *et al.* [9] and more recently by Zanuttigh *et al.* [14]. The emerging state of the art, based on the phase shifting algorithm, has been reviewed by Servin *et al.* in [11]. In the mean time, new approaches, like the Fourier-based regularized method of Legarda-Saenz and Espinosa-Romero [6], were developed which, however, could not compete with the state of the art.

Based on the phase shifting method, Mirdehghan *et al.* [7] recently presented a procedure to generate optimal scene-dependent projection patterns and thus to control the quality of the results. Zhang and Yau presented in [17] a system with two cameras that offers many quality advantages in contrast to standard setups with one camera and one projector. Based on this setup, the devices can be automatically calibrated without any user interaction, as demonstrated in [1] and [2].

Unfortunately, the recording time is the great weakness of the structured light method. One way to shorten the required acquisition time is to distribute several patterns among the different color channels of the cameras and projectors used ([5], [15]). These approaches work in theory but suffer from color cross-talk between cameras and projector and a very accurate color calibration is required. In particular, the object color influences the type and strength of the cross-talk. This leads to difficulties in implementing the procedures in practice and even then, one has to expect large quality losses.

To reduce the number of acquisitions required, Guan *et al.* [4] and Sansoni and Redaelli [10] combine patterns of different frequencies into individual patterns. Several fringes are encoded by carrier waves and additively combined. Afterwards they are separated by filter methods. These methods work in theory, but have a poor applicability in practice. The frequencies of the carrier waves must be stable in the image to enable an appropriate extraction. Nevertheless, they made it possible for the first time to provide information in the decoded direction of the patterns. Based on this idea, Yang *et al.* [13] further improved this approach, and created special patterns based on co-prime frequent sine waves that can be more robustly separated by a Garbor filter. Recent advances in real-time measurement with structured light have been detailed and analyzed by Zhang in [16]. Finally, Wang and Yang [12] recently introduced a one-shot approach based on binary stripe patterns, from which the phase can be directly approximated and interpolated. However, the approach assumes the stripes to be continuously visible in the scene, which cannot be guaranteed for general scenarios.

All in all, the problem of combining multiple patterns has already been mentioned, but has not been solved satisfactorily, yet. In particular, the combination of horizontal and vertical patterns has not yet been addressed, before.

3 Mathematical Investigation

In order to develop a new projection pattern, that allows to simultaneously recover the horizontal and vertical phases, we first examine the standard case more closely. This investigation will provide new insights into the amplitude of the superposition of the illuminated scene. These findings will finally enable a subsequent separation of the phase directions from the combined patterns.

3.1 Background: Sinusoidal Phase Shifting Method

Basis of the presented work is the *sinusoidal phase shifting* method. Thereby, patterns are modulated by sine or cosine (convention-dependent) signals and equidistantly shifted at least three times over the periodic domain. The patterns are projected onto the scene and captured by the cameras. Superposition of the resulting images allows to encoded the scene texture-invariant. Horizontal and vertical directions are treated by separate sets of patterns, each modulated by a sine/cosine in the respective direction and continued constantly in the other direction. Horizontal and vertical sets of patterns P_n^H and P_n^V with frequencies F_H and F_V that are shifted $n = 1, ..., N$ times, can be explicitly generated as:

$$P_n^H(i,j) \coloneqq \cos\left(\frac{2\pi j}{width}F_H + \frac{2\pi(n-1)}{N}\right),\ P_n^V(i,j) \coloneqq \cos\left(\frac{2\pi i}{height}F_V + \frac{2\pi(n-1)}{N}\right) \quad (1)$$

Thereby, $i = 1, ..., height$ and $j = 1, ..., width$ denote the image pixels. The first row of Figure 1 shows an exemplary set of horizontal (a) and vertical (b) patterns with $N = 3$ and $F_H = F_V = 1$. In both cases, the patterns are shown to the left, and the projection of the patterns onto an exemplary scene is shown to the right.

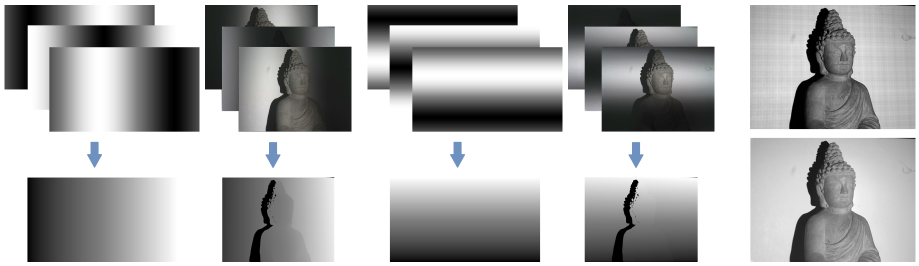

(a) Horizontal phase recovery (b) Vertical phase recovery (c) Amplitudes

Fig. 1: Example of the phase shifting algorithm for encoding a scene by phase recovery via harmonic addition theorem. The top rows of (a) and (b) show sets of horizontal and vertical fringe patterns and the resulting scene after projection. The bottom rows show the phase images computed by Eq. (3). (c) shows the amplitude of the superposition (Eq. (4)) (top) and the one given by the scaled texture as introduced in Lemma 1 (bottom).

Harmonic Addition Theorem Structured light approaches with sinusoidal patterns are based on practical application of the *harmonic addition theorem* (see [8]). It states that any superposition of cosines with same phase is again a cosine with the same phase:

$$\sum_{n=1}^{N} I_n \cos(\delta_n) = A \cos(\Phi) \tag{2}$$

$$\text{with} \quad \Phi = \text{atan2}\left(\sum I_n \sin(\delta_n),\ \sum I_n \cos(\delta_n)\right) \tag{3}$$

$$\text{and} \quad A^2 = \sum_{n=1}^{N} \sum_{m=1}^{N} I_n I_m \cos(\delta_n - \delta_m)\ , \tag{4}$$

where δ_n, δ_m denote the equidistant phase shifts, Φ the phase to be recovered and A the amplitude of the superposition. atan2 denotes the two-dimensional arcustangens function taking into account the quadrants of the input.

Recovering the Phases in the Scene Projecting patterns from Equation (1) to a scene I results in images I_n^H and I_n^V for the different phase shifts $n = 1, ..., N$. Applying Equation (3), the horizontal and vertical phases Φ_H and Φ_V can then be computed by:

$$\begin{aligned} \Phi_H &= \text{atan2}\left(\sum I_n^H \sin(\delta_n),\ \sum I_n^H \cos(\delta_n)\right) \\ \Phi_V &= \text{atan2}\left(\sum I_n^V \sin(\delta_n),\ \sum I_n^V \cos(\delta_n)\right) \end{aligned} \tag{5}$$

The second rows of Figure 1 (a) and (b) show the recovered phases computed for the patterns and the scene. Using this information, the scene points are uniquely encoded by their horizontal and vertical phase values. This allows robust and dense matches between the different camera views and the projector to be achieved. Amplitude A is not needed here and therefore not treated further in literature. For the method that is developed in this work, A plays an important role and is therefore further investigated.

3.2 Amplitude of Superposition

From illuminated images I_n, amplitude A is given by Equation (4), which can be directly expressed in terms of a captured texture image I of the scene:

Lemma 1. *A captured scene I_n, illuminated by fringe patterns $P_n = sin(x+\delta_n)$, with an arbitrary number of equidistant shifts $n = 1, ..., N \geq 2$, can be superposed to*

$$\sum_{n=1}^{N} I_n \cos(\delta_n) = \frac{N}{4} I \cos(\Phi) \;, \tag{6}$$

where Φ denotes the phase angle and I the fully illuminated scene.

Figure 1 (c) shows the amplitudes of the example scene computed by Eq. (4) (top) and from scaled texture as in Lemma 1 (bottom). Apart from artifacts caused by clipping (due to limited dynamic range of the cameras) and gamma corrections of the devices, these are identical. The lemma can be proved straight forward using properties of trigonometric functions and the harmonic addition theorem.

3.3 Combined Patterns

We are now going to introduce additively combined patterns and setup a mathematical problem with the newly gathered information about the amplitude. Solving this problem enables the recovery of horizontal and vertical phase values simultaneously.
Let the combined patterns P_n^C be defined as

$$P_n^C := \frac{1}{2}(P_n^H + P_n^V) \quad \text{for } n = 1, ..., N. \tag{7}$$

Thereby, two-dimensional sinusoidal patterns result as visualized in Figure 2 (a, left) and projected to the scene (b, left). The shifting direction naturally becomes the diagonal. The task in the following is to extract the horizontal as well as the vertical phase simultaneously from images of the scene, illuminated by these patterns.

Assuming the optimal case, where cameras and projector linearly respond and do not perform any gamma correction or internal post-processing, a captured scene is proportional to the sum of the separately illuminated scenes I^H and I^V:

$$I^C = P^C \odot \frac{I}{2} = \frac{1}{2}(P^H + P^V) \odot \frac{I}{2} = \frac{1}{2}(I^H + I^V), \tag{8}$$

where $\odot$ denotes pixel-wise multiplication of the patterns and the scene appearance I.

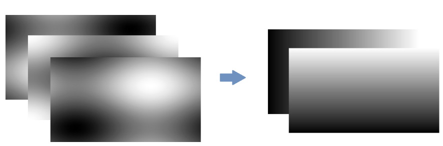

(a) Ideal phases computed from patterns

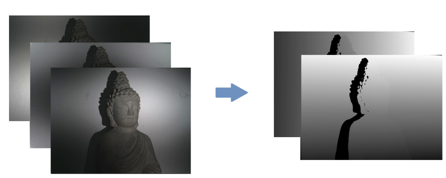

(b) Scene phases from camera images

Fig. 2: Combined sinusoidal patterns, computed by Equation (7) and projected onto the scene. The horizontal and vertical phases, to be recovered, are shown to the right.

Problem Formulation With Lemma 1 and Equation (8), we directly get the basic properties to set up the problem to be solved, in order to extract the phase information:

$$\begin{aligned} 2\sum_{n=1}^{N} I_n^C \cos(\delta_n) &= \frac{N}{4} I \cos(\Phi_H) + \frac{N}{4} I \cos(\Phi_V) \\ 2\sum_{n=1}^{N} I_n^C \sin(\delta_n) &= \frac{N}{4} I \sin(\Phi_H) + \frac{N}{4} I \sin(\Phi_V) \end{aligned} \tag{9}$$

This gives us two equations of two phase values, that have to be recovered from the superpositions per pixel. In the following section we treat the problem strictly mathematically, before we apply it again to the real world.

3.4 Mathematical Solution to the Problem

Given the following system of equations:

$$\begin{aligned} a\cos(x) + a\cos(y) &= b \\ a\sin(x) + a\sin(y) &= c \end{aligned} \tag{10}$$

with measured data a, b, c, we want to compute optimal values x, y solving both equations. Using addition theorems of trigonometric functions and dividing leads to:

$$\begin{aligned} 2a\cos(\frac{x}{2} + \frac{y}{2})\cos(\frac{x}{2} - \frac{y}{2}) &= b \\ 2a\sin(\frac{x}{2} + \frac{y}{2})\cos(\frac{x}{2} - \frac{y}{2}) &= c \end{aligned} \quad \Rightarrow \quad x + y = 2\arctan\left(\frac{c}{b}\right) \tag{11}$$

Therefore, we can decouple the equations of (11). Both are leading to the same equation:

$$2ab\cos(z) + 2ac\sin(z) = b^2 + c^2 \quad z \in \{x, y\} \tag{12}$$

Using harmonic addition theorem, four explicit solutions for this equation can be derived, where the two feasible ones are given by

$$x/y = 2\arctan\left(\frac{2ac \pm \sqrt{(b^2 + c^2)(4a^2 - b^2 - c^2)}}{b^2 + 2ab + c^2}\right) . \tag{13}$$

4 Application to Real World

The left column of Figure 3 shows the results of Equation (13) applied to the system (9) that models the real process. If there is a significant influence of ambient light, it may be necessary to subtract an ambient image from the captured images.

With the proposed procedure, phase values Φ_H and Φ_V can be recovered robustly. Unfortunately, due to the symmetric additive superposition of the phases in the whole procedure we do not have any information about which of the two phase values corresponds to the horizontal and which to the vertical one. These interchanges can occur

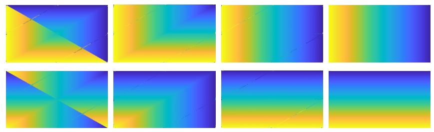

(a) Basic level of synthetic data set ($F_H = 1$, $F_V = 1$)

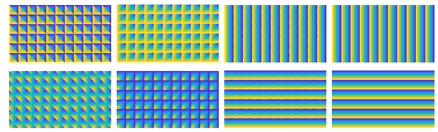

(b) Higher level of synthetic data set ($F_H = 11$, $F_V = 6$)

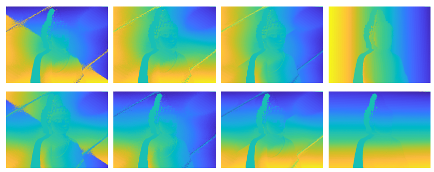

(c) Basic level of real captured data set ($F_H = 1$, $F_V = 1$)

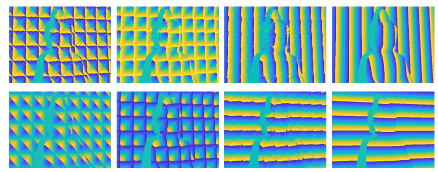

(d) Higher level of real data set ($F_H = 11$, $F_V = 6$)

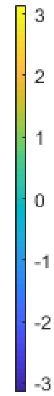

Fig. 3: Results of the algorithm applied to synthetic and real data for different frequencies. For each set the two rows show the horizontal and the vertical phase. The left two columns show the results of formula (13) before and after the *comparison step*. The third column shows the phase after the *swapping step*. The ground truth is depicted in the right column. The colorbar indicates the color coding in the range of $[-\pi, \pi]$.

at pixel level due to the pixel-wise approach. However, due to the natural continuity of the phases, these interchanges usually occur fragmentary. This can be seen in the first columns of the different examples of Figure 3 for different frequencies, for both the synthetic and the real case. Note that application directly to the patterns is meaningful for any synthetic scene, through the scene-independent pixel-wise approach.
The first errors can be corrected by simple comparison (*comparison step*), which sorts the values to fragments, lifting the swaps from pixel to region level:

$$\varPhi_H = \max\{\varPhi_H, \varPhi_V\}\ , \quad \varPhi_V = \min\{\varPhi_H, \varPhi_V\} \tag{14}$$

The second columns of Figure 3 (a,b,c,d) show the effect to the respective scenes.

4.1 Swapping Step

After this step, still many values are swapped (see Figure 3). A gradient based strategy could be used to sort them, which would not be per-pixel and therefore scene dependent.

A common procedure, to obtain reconstructions of high accuracy, is the projection of several levels of fringe images with increasing frequencies. It is assumed that separate horizontal and vertical fringe images recorded at frequency 1 were projected in the first level, so that basic phases are available. In order to get a more applicable swapping procedure, that is per-pixel and stable in difficult situations (e.g. discontinuities in the phase) this can be done during the phase unwrapping of the higher level phases. We present a simple pixel-wise unwrapping strategy, that can be used to perform the swapping step simultaneously by checking for consistency with the recorded images.

Per Pixel Unwrapping using Predicted Phase Assume we have computed a wrapped phase $\hat{\Phi}$ from fringes with some frequency F and a predicted phase Φ_0 of a previous level, that is not wrapped. A refined phase Φ can be computed by unwrapping $\hat{\Phi}$ using information from Φ_0. In a perfect world the following equation would hold true:

$$F \cdot \Phi = \hat{\Phi} + k \cdot 2\pi, \qquad k \in \mathbb{Z}_{\geq 0} \tag{15}$$

In a scenario with carefully increased frequencies, one can at least assume that there are no jumps larger than π from one level to the next one, which means

$$\hat{\Phi} + k \cdot 2\pi - F \cdot \Phi_0 \leq \pi \quad \Rightarrow \; k = \left\lfloor \frac{F \cdot \Phi_0 - \hat{\Phi} + \pi}{2\pi} \right\rfloor \tag{16}$$

with floor rounding $\lfloor \cdot \rfloor$. Therefore, $\hat{\Phi}$ can be explicitly unwrapped to Φ by:

$$\Phi = \frac{\hat{\Phi}}{F} + \frac{2\pi}{F} \left\lfloor \frac{F \cdot \Phi_0 - \hat{\Phi} + \pi}{2\pi} \right\rfloor \tag{17}$$

Per Pixel Swapping Using the per pixel unwrapping, we can perform the unwrapping step as well on the phase combination (Φ_H, Φ_V) as on the swapped one (Φ_V, Φ_H). The consistency towards captured fringe images can be described by a suitable error like:

$$E_n(\Phi_H, \Phi_V) = \left| \big(\cos(F^H \Phi_H + \delta_n) + \cos(F^V \Phi_V + \delta_n) + 2 \big) I - 4 I_n^C \right|.$$

Since we can assume the refined phases to improve after every unwrapping step, the accumulated consistency error of all captured images should decrease. Therefore, the combination with lower consistency error can be chosen to complete the swapping.

Level	1	2	3	4
Combined Patterns				
Median Error of Φ_H	0.0514	0.0149	0.0066	0.0028
Median Error of Φ_V	0.0587	0.0390	0.0124	0.0055
Captured Images	6	9	12	15
Separate Patterns				
Median Error of Φ_H	0.0514	0.0110	0.0052	0.0019
Median Error of Φ_V	0.0587	0.0278	0.0093	0.0034
Captured Images	6	12	18	24

Table 1: Median errors for different levels of the proposed method with combined patterns and separate patterns, applied to the example data.

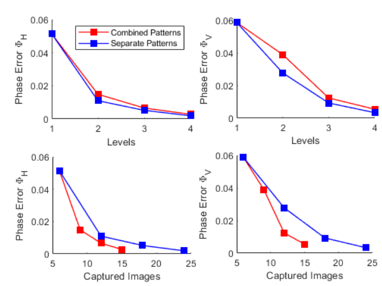

Fig. 4: Behavior of the median phase error with respect to the images that have to be captured.

5 Evaluation

In order to evaluate the behavior of the procedure, we have drawn the median pixel error of the calculated phases to the ground truth after several levels in Table 1, as well for the

(a) Ground truth and Φ_H computed (b) Ground truth and Φ_V computed

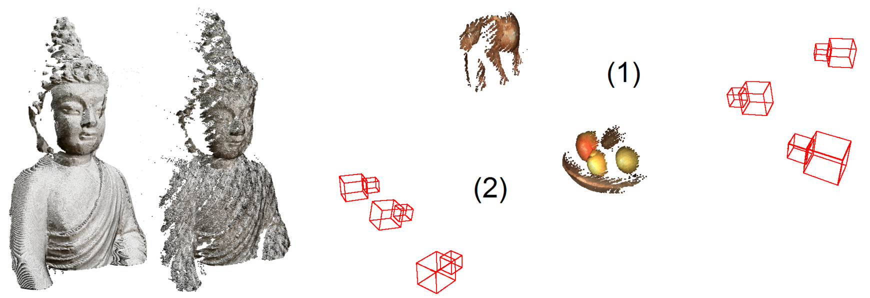

(c) Reconstructed point clouds (d) Auto-calibrations received from the correspondences

Fig. 5: Ground truth phases of the exemplary scene (a, b, left) in comparison to the recovered phases (a, b, right). The triangulated point clouds from ground truth (left) and simultaneously recovered phase (right) are shown in (c). Auto-calibrations from point correspondences of two additional scenes are visualized in (d).

proposed approach with combined patterns as for the separate approach. As expected, the error of the combined phases in each level is slightly higher than the separate procedure with separately computed horizontal and vertical phases. However, less recordings were necessary. Considering the accuracy in relation to the image captures used, even with a two-stage procedure and the 12 shots usually required for this, the combined procedure can take another level and double the accuracy of the calculated phases (see Fig. 4). Figure 5 shows the final phases, computed by the proposed approach, in comparison to the ground truth. It should be noted that the gamma correction of the devices used (especially the projector) strongly influences the quality of later reconstructions, since it violates the assumed linearity condition from Equation (8). We have applied inverse gamma correction to the projected patterns with a roughly determined gamma value to compensate for this and can therefore demonstrate real results. Nevertheless, the use of industrial projectors without gamma correction or precise gamma calibration of the consumer device used, would significantly improve the quality of the reconstructions. Finally, the calibration results of two other setups and scenes, directly computed from the received point correspondences are visualized in Figure 5 (d).

6 Conclusions

A new method has been introduced, which allows to perform sinusoidal structured light encoding in horizontal and vertical directions, at the same time. Thereby, the recording time is effectively halved. This procedure especially allows to auto-calibrate arbitrary setups directly from the achieved point correspondences. Extensive mathematical investigations were carried out, which yield important new findings in the field of applied harmonic addition theorem. Overall, a method was developed, which can determine the horizontal and vertical phase values from the combined captured patterns pixel-wise, making it scene-independent and therefore applicable to a wide variety of scenarios. The applicability to real scenes besides artificial ones was demonstrated as well. The results are highly interesting both mathematically and from a computer vision point of view, as they open up new possibilities in the field.

References

1. Fetzer, T., Reis, G., Stricker, D.: Robust auto-calibration for practical scanning setups from epipolar and trifocal relations. In: 2019 16th International Conference on Machine Vision Applications (MVA). pp. 1–6. IEEE (2019)
2. Fetzer, T., Reis, G., Stricker, D.: Stable intrinsic auto-calibration from fundamental matrices of devices with uncorrelated camera parameters. In: 2020 IEEE Winter Conference on Applications of Computer Vision (WACV). IEEE (2020)
3. Fetzer, T., Reis, G., Stricker, D.: Fast projector-driven structured light matching in sub-pixel accuracy using bilinear interpolation assumption. In: International Conference on Computer Analysis of Images and Patterns. Springer (2021)
4. Guan, C., Hassebrook, L., Lau, D.: Composite structured light pattern for three-dimensional video. Optics Express **11**(5), 406–417 (2003)
5. Je, C., Lee, S.W., Park, R.H.: Color-phase analysis for sinusoidal structured light in rapid range imaging. arXiv preprint arXiv:1509.04115 (2015)
6. Legarda-Saenz, R., Espinosa-Romero, A.: Wavefront reconstruction using multiple directional derivatives and fourier transform. Optical Engineering **50**(4), 040501 (2011)
7. Mirdehghan, P., Chen, W., Kutulakos, K.N.: Optimal structured light à la carte. In: Proceedings of the IEEE Conference on Computer Vision and Pattern Recognition (2018)
8. Oo, N., Gan, W.S.: On harmonic addition theorem. International Journal of Computer and Communication Engineering **1**(3), 200 (2012)
9. Salvi, J., Fernandez, S., Pribanic, T., Llado, X.: A state of the art in structured light patterns for surface profilometry. Pattern recognition **43**(8), 2666–2680 (2010)
10. Sansoni, G., Redaelli, E.: A 3d vision system based on one-shot projection and phase demodulation for fast profilometry. Measurement Science and Technology **16**(5), 1109 (2005)
11. Servin, M., Estrada, J., Quiroga, J.A.: The general theory of phase shifting algorithms. Optics express **17**(24), 21867–21881 (2009)
12. Wang, Z., Yang, Y.: Single-shot three-dimensional reconstruction based on structured light line pattern. Optics and Lasers in Engineering **106**, 10–16 (2018)
13. Yang, L., Li, F., Xiong, Z., Shi, G., Niu, Y., Li, R.: Single-shot dense depth sensing with frequency-division multiplexing fringe projection. Journal of Visual Communication and Image Representation **46**, 139–149 (2017)
14. Zanuttigh, P., Marin, G., Dal Mutto, C., Dominio, F., Minto, L., Cortelazzo, G.M.: Time-of-flight and structured light depth cameras. Technology and Applications pp. 978–3 (2016)
15. Zhang, L., Curless, B., Seitz, S.M.: Rapid shape acquisition using color structured light and multi-pass dynamic programming. In: Proceedings. First International Symposium on 3D Data Processing Visualization and Transmission. pp. 24–36. IEEE (2002)
16. Zhang, S.: Recent progresses on real-time 3d shape measurement using digital fringe projection techniques. Optics and lasers in engineering **48**(2), 149–158 (2010)
17. Zhang, S., Yau, S.T.: Three-dimensional shape measurement using a structured light system with dual cameras. Optical Engineering **47**(1), 013604 (2008)